

Role of *N*-donor groups on the stability of hydrazone based hypercoordinate silicon(IV) complexes: Theoretical and experimental perceptions



Pothini Suman^a, Sannapaneni Janardan^a, Mohsin Y. Lone^b, Prakash Jha^b, Kari Vijayakrishna^a, Akella Sivaramakrishna^{a,*}

^a Department of Chemistry, School of Advanced Sciences, VIT University, Vellore 632 014, TN, India

^b School of Chemical Sciences, Central University of Gujarat, Sector-30, Gandhinagar, Gujarat, India

ARTICLE INFO

Article history:

Received 17 April 2015

Accepted 5 August 2015

Available online 24 August 2015

Keywords:

Pentacoordinate siliconium salts

Thermal stability

Phosphinimino ligand

DFT calculations

Ligand crossover reaction

ABSTRACT

A triphenylphosphinimino donor group is illustrated as a ligand in pentacoordinate siliconium halide dichelates, $[YSiL_2]^+X^-$, where L is the bidentate ligand $-OC(R)=NN=PPh_3-$ ($R = t\text{-Bu-Ph}$ or Ph), $Y = Me$, Ph , CH_2Cl , $CHCl_2$, Cl or Br , and $X = Cl$ or Br . All the new complexes were characterized by NMR spectroscopy and elemental analysis. The remote substituent, the *t*-Bu-phenyl or phenyl group, imparts more pentacoordinate character, i.e. more ionization to the complexes, compared to the $PhCH_2$ group. DFT calculations indicate that the central silicon atom, due to the more positive charge, demands greater electron density. As a result of this, shorter Si–O, Si–N and Si–Cl bonds were observed. Both theoretical and experimental analysis indicate that the phosphinimino ligand is a stronger donor than the previously studied dimethylamino and isopropylideneimino ligands, causing all of the complexes to be pentacoordinate siliconium-halide salts in solution. The hypercoordinate silicon dichelates undergo unique intermolecular chelate exchange reactions: (i) complete ligand transfer from the dichelates to $PhSiCl_3$ by a ligand priority order and (ii) bidentate ligand interchange between the dichelates and a trimethylsilyl-hydrazone precursor. Thermolysis of some selected hypercoordinated silicon(IV) complexes containing a silicon–carbon σ -bond significantly undergo a two step decomposition, while other complexes with silicon–halogen σ -bonds follow three steps. The thermal decomposition strongly depends on the nature of the substituents directly attached to the central silicon atom.

© 2015 Elsevier Ltd. All rights reserved.

1. Introduction

The chemistry of hypercoordinate compounds has been acquiring wider and deeper attention both by organic chemists and by inorganic chemists due to their potential in developing pathways for the synthesis of chemicals which may otherwise be difficult to prepare or even be inaccessible [1]. Hypercoordinate silicon (IV) complexes are highly flexible molecular systems, undergoing a variety of chemical and geometrical transformations [2], including ionic dissociation, an alternative neutral dissociation of the $N \rightarrow Si$ dative bond [3,4], thermal and photochemical molecular rearrangements as well as flexible intramolecular ligand exchange reactions controlled by priority rules [5]. Apart from the rich chemistry of these penta and/or hexacoordinate silicon compounds, it has been found that these species are relatively cheap, have low

toxicity and are environmental friendly reagents [6,7] which makes them ideal to develop organocatalyzed enantio-selective reactions [8], similar to other organosilicon compounds [9]. Stereoselective reactions catalyzed by hypercoordinate silicate compounds have been very well-reviewed in the recent past [10].

Investigations on the effect of ligands upon the reactivity patterns of hypercoordinate silicon complexes led to the preparation and study of a new class of silicon complexes: those with a triphenylphosphinimino-*N* ligand group with the *t*-Bu-Ph substituent, which are the subject of the present work [11]. The new ligand was expected, and indeed was found, to be superior in terms of donor strength in comparison to other nitrogen-donor ligands (in **1**, **2** and **3**), due to its ylide character [12,13] and the resulting excess electron density on the nitrogen atom. The strength of the coordination also depends on the nature of the remote substituent 'R'. The evidence for complete intermolecular bidentate ligand crossover among different dichelate complexes is also discussed, further extending the flexible nature of these compounds, and this

* Corresponding author. Tel.: +91 416 2202351; fax: +91 416 2243092.

E-mail address: asrkrishna@vit.ac.in (A. Sivaramakrishna).

ligand crossover is controlled by priority rules. However, it has been widely unexplored whether there are some significant influences of the hypercoordinate Si atom's coordination environment through theoretical and experimental studies.

2. Experimental section

The reactions were carried out under dry argon using Schlenk techniques. Solvents were dried and purified by standard methods. Reagents (including polyhalosilanes) were purchased from Sigma–Aldrich. The halosilanes were distilled and kept in sealed ampules prior to use. NMR spectra were recorded on a Bruker Avance DMX-500 spectrometer operating at 500.13, 202.46, 125.76 and 99.36 MHz, respectively, for ^1H , ^{31}P , ^{13}C and ^{29}Si spectra. Spectra are reported in δ (ppm) relative to TMS, as determined from standard residual solvent–proton (or carbon) signals for ^1H and ^{13}C , relative to external (capillary) H_3PO_4 for ^{31}P , and directly from TMS for ^{29}Si . Melting points were measured in sealed capillaries using a Büchi melting point instrument and are uncorrected. TG curves in the range 25–900 °C were recorded using an EXSTAR TG/DTA 6300 instrument at a heating rate of 10 °C min^{-1} in a dynamic nitrogen atmosphere. In each experiment, solid samples having masses ranging from 9 mg to 10 mg were used.

2.1. Computational methodology

All the quantum chemical calculations of the Si complexes have been calculated using the Gaussian 09 program package [16]. The spin multiplicity of all the studied molecules is singlet, while the charge for **1** and **2** is zero and for **3**, **8**, **11** and **13** it is +1. Geometry minimization was carried out by employing Becke's three parameter hybrid density functional B3LYP [17–19] and valance triple- ζ 6-311G (d,p) as a basis set for all the atoms. Frequency calculations were exercised to ascertain the stationary structures. Natural bond orbital (NBO) [20,21] analysis was carried out at the B3LYP/6-311G (d,p) level by the NBO 3.1 version of Gaussian 09 [16]. ^{29}Si NMR shielding constants were computed at the DFT level by using the gauge independent atomic orbitals (GIAO) [22] method in conjunction with the meta-GGA functional HCTH. The choice of functional was made from the literature [23]. The effect of solvent on shielding constants was accounted for by using the polarizable continuum model (PCM) of Tomasi and co-workers [24]. Pople's triple zeta, split valance basis set 6-311 + G(2d) was employed for the calculation of shielding constants.

2.2. Materials and methods

All reactions were carried out under an inert atmosphere of dry nitrogen using standard Schlenk and vacuum line techniques. The polyhalosilanes, Me_3SiCl , 4-(*t*-butyl)benzohydrazide and benzohydrazide were purchased from Sigma Aldrich and used as such. The solvents were purchased from Sd fine chemicals purified and distilled according to standard procedures prior to use.

2.3. Preparation of compounds

2.3.1. 4-(*t*-Butyl)-*N*-(triphenylphosphoranylidene)benzohydrazide (**6**)

At ice-cold temperature, 8.01 g (50.3 mmol) of Br_2 in 50 mL of CCl_4 was added dropwise to a solution of 12.02 g (45.7 mmol) of Ph_3P in 100 mL of CCl_4 and the mixture was allowed to stir for 4 h. The resultant product (Ph_3PBr_2) which formed was in the form of a pale yellow precipitate and this was used for further reaction without isolation. 4-(*t*-Butyl)benzohydrazide (8.79 g, 23.6 mmol) was added to the reaction mixture, followed by dropwise addition of 10.62 g (105.2 mmol) of triethylamine in 80 mL of

CCl_4 . The mixture was stirred for 14 h at room temperature and then the precipitate which formed was filtered off and dissolved in CHCl_3 ; $\text{Et}_3\text{N}\cdot\text{HBr}$ was washed out with cold water in a separating funnel. The solid isolated on evaporation of CHCl_3 was dried under vacuum to yield 13.85 g (67%) of **6**. M.p.: 186–188 °C. ^1H NMR (CDCl_3 , 300 K) δ , ppm: 1.239 (s, 9H, CH_3), 7.35–7.60 (m, 19H, Ph); ^{13}C NMR (CDCl_3 , 300 K) δ , ppm: 31.14 (CH_3), 34.95 (C- Me_3), 125.60–132.15 (Ph), 168.63 (C=O); ^{31}P NMR (CDCl_3 , 300 K) δ , ppm: 29.6.

2.3.2. *O*-Trimethylsilyl-*N*-(triphenylphosphinimino)-4-(*t*-butyl)benzohydrazide (**7**)

To a mixture of 8.04 g (17.7 mmol) of **6** and 2.24 g (22.2 mmol) of triethylamine in 100 mL of diethyl ether, Me_3SiCl (2.74 g, 25.2 mmol) in 10 mL of diethyl ether was added dropwise. After refluxing for 10 h, the mixture was cooled and $\text{Et}_3\text{N}\cdot\text{HCl}$ was filtered off, followed by the removal of volatiles at low pressure. The white powder that formed was washed with 15 mL of *n*-hexane and filtered, yielding 3.94 g (42%) of **7**. ^1H NMR (CDCl_3 , 300 K) δ , ppm: 0.57 (s, 9H, SiCH_3), 1.23 (s, 9H, CCH_3), 7.33–7.86 (m, Ph); ^{31}P NMR (CDCl_3 , 300 K) δ , ppm: 16.2; ^{29}Si NMR (CDCl_3 , 300 K) δ , ppm: 7.2.

2.3.3. Bis[*N*-(triphenylphosphinimino)-4-*t*-butyl-phenyl-*N'*,*O*]methylsiliconium chloride (**8**)

To a mixture of 0.494 g (0.93 mmol) of **7** in 10 mL of chloroform, MeSiCl_3 (0.31 g, 2.11 mmol) was added, followed by stirring at room temperature for 30 min. The residue left after removal of volatiles under reduced pressure was recrystallized from a solvent mixture of 1:2 CH_2Cl_2 –*n*-hexane. The product was washed with 10 mL of *n*-hexane. The yield was 0.43 g (93%) of a white powder. M.p.: 106–108 °C. ^1H NMR (CDCl_3 , 300 K) δ , ppm: 0.794 (s, 3H, Si-CH_3), 1.16 (s, 18H, CH_3), 7.38–7.90 (m, 38H, Ph); ^{13}C NMR (CDCl_3 , 300 K) δ , ppm: 8.47 (Si-CH_3), 25.68 (Me_3), 31.95 (C- Me_3), 126.83–132.94 (Ph), 155.33 (C=N); ^{31}P NMR (CDCl_3 , 300 K) δ , ppm: 41.2; ^{29}Si NMR (CDCl_3 , 300 K) δ , ppm: –77.1.

2.3.4. Bis[*N*-(triphenylphosphinimino)-4-*t*-butyl-phenyl-*N'*,*O*]chloromethylsiliconium chloride (**9**)

In a Schlenk flask, $\text{CH}_2\text{ClSiCl}_3$ (0.28 g, 1.30 mmol) was added to a mixture of 0.373 g (0.70 mmol) of **7** in 10 mL of chloroform, followed by stirring at room temperature for 30 min. The same procedure as mentioned above for 2.3.3 was used for the work-up of the reaction mixture and further purification of the product. The yield was 0.32 g (88%) of a white powder. M.p.: 114 °C. ^1H NMR (CDCl_3 , 300 K) δ , ppm: 0.81 (s, 18H, CH_3), 2.11, 2.38 (ABq, $^2J_{\text{AB}} = 14.4$ Hz, 2H, CH_2Cl), 6.28–7.72 (m, 38H, Ph); ^{13}C NMR (CDCl_3 , 300 K) δ , ppm: 27.48 (CH_3), 31.29 (C- Me_3), 64.96 (CH), 121.94–121.24 (Ph), 158.67 (C=N); ^{31}P NMR (CDCl_3 , 300 K) δ , ppm: 52.2; ^{29}Si NMR (CDCl_3 , 300 K) δ , ppm: –94.1.

2.3.5. Bis[*N*-(triphenylphosphinimino)-4-*t*-butyl-phenyl-*N'*,*O*]dichloromethylsiliconium chloride (**10**)

A Schlenk flask was charged with 0.512 g (0.97 mmol) of **7** in 10 mL of chloroform and SiCl_3 (0.29 g, 1.62 mmol) and the mixture was then stirred at room temperature for 30 min. The same procedure as mentioned above for 2.3.3 was used for the work-up of the reaction mixture and further purification of the product. The yield was 0.45 g (92%) of a white powder. M.p.: 72–74 °C (dec). ^1H NMR (CDCl_3 , 300 K) δ , ppm: (s, 18H, CH_3), 7.35–7.60 (m, 38H, Ph); ^{13}C NMR (CDCl_3 , 300 K) δ , ppm: 28.14 (CH_3), 31.95 (C- Me_3), 48.78 (CH_2), 122.60–129.89 (Ph), 156.80 (C=N); ^{31}P NMR (CDCl_3 , 300 K) δ , ppm: 47.6; ^{29}Si NMR (CDCl_3 , 300 K) δ , ppm: –88.6.

2.3.6. Bis[*N*-(triphenylphosphinimino)-4-*t*-butyl-phenyl-*N'*,*O*]phenylsiliconium chloride (**11**)

PhSiCl₃ (0.301 g, 1.42 mmol) was added to a solution of 0.375 g (0.71 mmol) of **7** in 10 mL of chloroform, followed by stirring at room temperature for 30 min. The same procedure as mentioned above for 2.3 was used for the work-up of the reaction mixture and further purification of the product. The yield was 0.32 g (87%) of a colourless solid. M.p.: 94–96 °C (dec). ¹H NMR (CDCl₃, 300 K) δ, ppm: 1.76 (s, 18H, CH₃), 6.90–7.74 (m, 38H, Ph); ¹³C NMR (CDCl₃, 300 K) δ, ppm: 25.66 (CH₃), 30.37 (C-Me₃), 125.58–134.32 (Ph), 157.26 (C=N); ³¹P NMR (CDCl₃, 300 K) δ, ppm: 45.8; ²⁹Si NMR (CDCl₃, 300 K) δ, ppm: –92.7.

2.3.7. Bis[*N*-(triphenylphosphinimino)-4-*t*-butyl-phenyl-*N'*,*O*]chlorosiliconium chloride (**12**)

To a mixture of 0.71 g (1.36 mmol) of **7** in 10 mL of chloroform, SiCl₄ (0.32 g, 1.89 mmol) was added, followed by stirring at room temperature for 30 min. The same procedure as mentioned above for 2.3.3 was used for the work-up of the reaction mixture and further purification of the product. The yield was 0.55 g (82%) of a white solid. M.p.: 88–90 °C (dec). ¹H NMR (CDCl₃, 300 K) δ, ppm: 1.11 (s, 18H, CH₃), 6.57–7.02 (m, 38H, Ph); ¹³C NMR (CDCl₃, 300 K) δ, ppm: 26.95 (CH₃), 30.75 (C-Me₃), 121.40–128.75 (Ph), 157.78 (C=N); ³¹P NMR (CDCl₃, 300 K) δ, ppm: 49.8; ²⁹Si NMR (CDCl₃, 300 K) δ, ppm: –99.2.

2.3.8. Bis[*N*-(triphenylphosphinimino)-4-*t*-butyl-phenyl-*N'*,*O*]bromosiliconium bromide (**13**)

To a mixture of 0.33 g (0.63 mmol) of **7** in 10 mL of chloroform, SiBr₄ (0.300 g, 0.86 mmol) was added, followed by stirring at room temperature for 30 min. The same procedure as mentioned above for 2.3.3 was used for the work-up of the reaction mixture and further purification of the product. The yield was 0.29 g (91%) of a colourless solid. M.p.: 78–80 °C (dec). ¹H NMR (CDCl₃, 300 K) δ, ppm: 1.04 (s, 18H, CH₃), 6.707–7.60 (m, 38H, Ph); ¹³C NMR (CDCl₃, 300 K) δ, ppm: 27.13 (CH₃), 30.93 (C-Me₃), 121.58–128.90 (Ph), 158.63 (C=N); ³¹P NMR (CDCl₃, 300 K) δ, ppm: 53.1; ²⁹Si NMR (CDCl₃, 300 K) δ, ppm: –106.2.

2.3.9. *N*-(Triphenylphosphoranylidene)benzohydrazide (**14**)

In a 2-necked 500 mL RB flask, 6.47 g (40.6 mmol) of Br₂ in 80 mL of CCl₄ was added dropwise to a solution of 9.52 g (36.2 mmol) of Ph₃P in 120 mL of CCl₄ at 0 °C and the mixture was then stirred for 4 h. The resultant pale yellow precipitate, Ph₃PBr₂, was used as such in the subsequent reaction. Benzohydrazide (2.7 g, 36.3 mmol) was added to the reaction mixture followed by dropwise addition of 10.18 g (100.5 mmol) of triethylamine in 80 mL of CCl₄. The mixture was stirred for 2 h at room temperature and then heated for 2 h at 70 °C. After cooling the precipitate that formed, it was filtered off and dissolved in CHCl₃, and Et₃N·HBr was washed out with ice-cold water in a separating funnel. The solid isolated on evaporation of CHCl₃ was dried under vacuum to yield 6.45 g (83%) of **14**. M.p.: 206–208 °C. ¹H NMR (CDCl₃, 300 K) δ, ppm: 7.12–7.94 (m, 20H, Ph), 8.72 (s (broad), 1H, NH); ¹³C NMR (CDCl₃, 300 K) δ, ppm: 31.14 (CH₃), 34.95 (C-Me₃), 119.60–132.15 (Ph), 171.6 (NC=O); ³¹P NMR (CDCl₃, 300 K) δ, ppm: 29.2. *Anal. Calc.* for C₂₅H₂₁N₂O: C, 75.74; H, 5.34; N, 7.07. *Found:* C, 75.78; H, 5.41; N, 7.1%.

2.3.10. *O*-Trimethylsilyl-*N*-(triphenylphosphinimino)benzohydrazide (**15**)

5.24 g (13.22 mmol) of **14** and 1.52 g (15.02 mmol) of triethylamine in 100 mL of diethylether were added to a 3-necked RB flask. To this mixture, Me₃SiCl (1.63 g, 15.02 mmol) in 20 mL of diethyl ether was added dropwise. After refluxing for 8 h, the mixture was cooled and Et₃N·HCl was filtered off, followed by removal

of volatiles at low pressure. The white precipitate that formed was washed with 15 mL of *n*-hexane and filtered, yielding 4.24 g (68%) of **15**, consisting of a 2:1 mixture of *E*, *Z* isomers. ¹H NMR (CDCl₃, 300 K) δ, ppm: major isomer 0.08 (s, 9H, Si-CH₃), 7.12–7.78 (m, Ph); minor isomer 0.16 (s, 9H, Si-CH₃), 7.12–7.78 (m, Ph). ¹³C NMR (CDCl₃, 300 K) δ, ppm: major isomer 0.12 (Si-CH₃), 122.5–136.8 (Ph), 159.4 (N=C-O); minor isomer 1.9 (Si-CH₃), 122.5–136.8 (Ph), 147.3 (N=C-O). ³¹P NMR (CDCl₃, 300 K) δ, ppm: major isomer 17.2; minor isomer 19.4. ²⁹Si NMR (CDCl₃, 300 K) δ, ppm: major isomer 17.4; minor isomer 15.3. *Anal. Calc.* for C₂₈H₂₉N₂O₂PSi: C, 77.77; H, 6.24; N, 5.98. *Found:* C, 77.82; H, 6.33; N, 6.04%.

2.3.11. Bis[*N*-(triphenylphosphinimino)-phenyl-*N'*,*O*]methylsiliconium chloride (**16**)

MeSiCl₃ (0.11 g, 0.75 mmol) was added to a solution of **15** (0.286 g, 0.61 mmol) in 10 mL of chloroform, followed by stirring at room temperature for 30 min. The same procedure as mentioned above for 2.2.3 was used for the work-up of the reaction mixture and further purification of the product. The yield was 0.254 g (95%) of a white powder. M.p.: 154–56 °C. ¹H NMR (CDCl₃, 300 K) δ, ppm: 0.82 (s, 3H, Si-CH₃), 7.22–7.98 (m, 40H, Ph); ¹³C NMR (CDCl₃, 300 K) δ, ppm: 8.54 (Si-CH₃), 123.1–134.8 (Ph), 156.4 (O-C=N); ³¹P NMR (CDCl₃, 300 K) δ, ppm: 40.6; ²⁹Si NMR (CDCl₃, 300 K) δ, ppm: –76.2. *Anal. Calc.* for C₅₁H₄₃N₄O₂P₂SiCl: C, 70.46; H, 4.99; N, 6.44. *Found:* C, 70.52; H, 5.08; N, 6.52%.

2.3.12. Bis[*N*-(triphenylphosphinimino)-phenyl-*N'*,*O*]phenylsiliconium chloride (**17**)

PhSiCl₃ (0.1802 g, 0.85 mmol) was added to a solution of **15** (0.304 g, 0.65 mmol) in 10 mL of chloroform, followed by stirring at room temperature for 30 min. The same procedure was followed to work-up the reaction mixture as mentioned above. The yield was 0.28 g (93%) of a pale yellow solid. M.p.: 134–36 °C (dec). ¹H NMR (CDCl₃, 300 K) δ, ppm: 6.90–7.74 (m, 45H, Ph); ¹³C NMR (CDCl₃, 300 K) δ, ppm: 122.5–136.2 (Ph), 157.6 (O-C=N); ³¹P NMR (CDCl₃, 300 K) δ, ppm: 47.3; ²⁹Si NMR (CDCl₃, 300 K) δ, ppm: –94.3. *Anal. Calc.* for C₅₆H₄₅N₄O₂P₂SiCl: C, 72.21; H, 4.87; N, 6.01. *Found:* C, 72.36; H, 5.01; N, 6.08.

The other complexes, bis[*N*-(dimethylamino)benzoimidato-*N*,*O*]phenylsiliconium chloride (**18**) [14] and bis[*N*-isopropylideneimino]benzoimidato-*N'*,*O*]phenylsiliconium chloride (**19**) [15], were prepared from the corresponding precursors *N*-(isopropylideneimino)benzoimidate and *N*-(isopropylideneimino)-*O*-(trimethylsilyl)benzoimidate as per the literature reports.

2.4. General procedure for ligand crossover reactions

The reaction of Eq. (1) was carried out by the addition of a 10–20% molar excess of PhSiCl₃ to a CDCl₃ solution of **16** with stirring under N₂ atm. at ambient temperature for 15 min. The disappearance of the ²⁹Si NMR signal of **16**, accompanied by the growth of the corresponding crossover product **17**, was monitored by NMR. MeSiCl₃ was formed, along with an excess of unreacted PhSiCl₃. To ensure that the exchange was complete and irreversible, this procedure was followed by the addition of a large excess of MeSiCl₃. No reversal of the reaction was detected. These complexes were characterized by their ¹H, ¹³C, ²⁹Si and ³¹P NMR spectra, but could not be isolated because of rapid equilibration with their precursors.

In a similar way, the reactions of Eqs. (2) and (3) were monitored by ²⁹Si NMR spectral data on reacting **18** or **19** with **15** in CDCl₃ solution. In both the cases, the appearance of a new signal at δ –94.3 indicates the formation of **17**.

3. Results and discussion

In a recent note, the introduction of a new chelating ligand system based on *N*-cyclohexylidene hydrazides was described [15b]. In the present study, we have prepared several new silicon compounds (**6–19**) based on the phosphinimino donor group ($-\text{N}=\text{PPh}_3$) and have studied their donor properties in comparison with the former chelates (**1** and **2**). In particular, we were interested in comparing the donor strengths of the two nitrogen-ligand systems (NMe_2 , $\text{N}=\text{CMe}_2$ and $\text{N}=\text{PPh}_3$), as given in Chart 1, and their effects on siliconium ion formation and stability. Four criteria for donor strength have been studied: the N–Si bond length by DFT calculations, the ^{29}Si chemical shifts, the ligand crossover behavior and thermal stability.

3.1. DFT calculations

The two factors that can potentially explain the differences in bond lengths are coordination number and charge on a metal atom. It is well documented in the literature that an increase in ligand coordination increases the bond lengths of Si–O and Si–N covalent and dative bonds, which could be seen by comparing the Wiberg index, reported in Tables 1–3 respectively. This can be further elucidated in that an increase in coordination number increases the electron density around the silicon atom, leading to a decrease in the overlap of the metal–ligand orbitals and hence changes in the bond lengths. On the other hand, there is an inverse trend of charge and bond length followed by the complexes of interest. For the same coordination number, the decrease in the NPA [20] charge on the metal atom decreases the bond length, with a notable effect on axially directed bonds (Tables 1 and 2). This fact can be supported by the reason that the decrease in charge on the silicon atom leads to an expansion of the valence orbital, which

Table 3

Bond lengths, NPA [20] charge distribution and Wiberg index [21] of **3**.

Atoms	1-Si	2-Cl	3-O	4-O	5-N	6-N
NPA charge	2.028	−0.414	−0.847	−0.847	−0.987	−0.987
Bond length (Å)		2.130	1.716	1.716	1.875	1.875
Wiberg index		0.773	0.547	0.547	0.489	0.489

in turn increases the overlap of the metal–ligand orbitals and decreases the bond length. Moreover, the magnitude of the covalent bond interactions between the central metal atom and the ipso atoms of the ligands can be envisaged from the quantum chemistry wave function based Wiberg bond index (Tables 1–3). In other words, the electrophilicity of the central metal atom diminishes with the decrease in charge and the nucleophilic inclination of the ligands towards the center also drops thus, augmenting the bond length.

It is very clear from Tables 1–3 that the central silicon atom, due to a greater positive charge (2.028), demands greater electron density. As a result of this, shorter Si–O, Si–N and Si–Cl bonds are observed. The DFT optimized structures of **1**, **2** and **3** are given in Figs. 1–3 respectively.

3.2. Synthesis and characterization of products

The *N*-triphenylphosphinimines **6** and **14** were prepared from the corresponding phenyl-benzohydrazide (**5**) and triphenylphosphine dibromide (**4**) as described previously for the benzhydrazide analogue [25]. They were then converted to the corresponding *O*-trimethylsilyl derivatives (**7** and **15**) by the reaction with trimethylsilyl chloride in the presence of Et_3N (Schemes 1 and 2).

The transsilylation reaction of **7** with excess YSiX_3 ($\text{Y} = \text{Me/Ph/CH}_2\text{Cl/CHCl}_2/\text{Cl/Br}$ and $\text{X} = \text{Cl/Br}$) afforded exclusively ionic

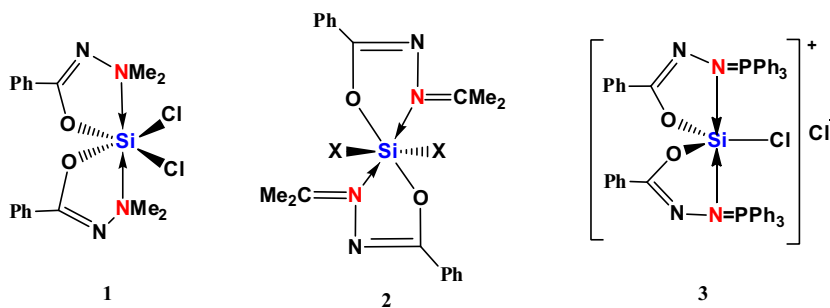


Chart 1.

Table 1

Bond lengths, NPA [20] charge distribution and Wiberg index [21] of **1**.

Atoms	1-Si	2-Cl	3-Cl	5-O	6-O	7-N	18-N
NPA charge	1.819	−0.447	−0.447	−0.837	−0.837	−0.432	−0.432
Bond length (Å)		2.207	2.207	1.783	1.783	2.061	2.061
Wiberg index		0.723	0.723	0.429	0.429	0.353	0.353

Table 2

Bond lengths, NPA [20] charge distribution and Wiberg index [21] of **2**.

Atoms	1-Si	4-Cl	5-Cl	6-O	7-O	8-N	9-N
NPA charge	1.779	−0.476	−0.464	−0.823	−0.823	−0.422	−0.422
Bond length (Å)		2.252	2.220	1.764	1.764	1.973	1.973
Wiberg index		0.669	0.692	0.448	0.448	0.416	0.416

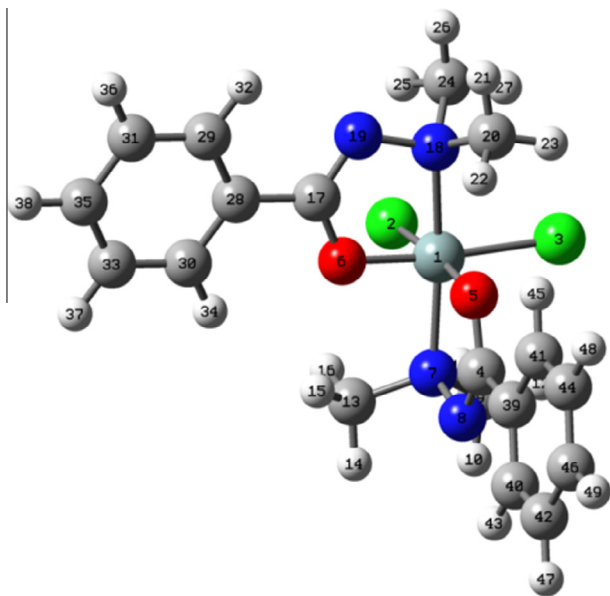


Fig. 1. DFT optimized structure of 1.

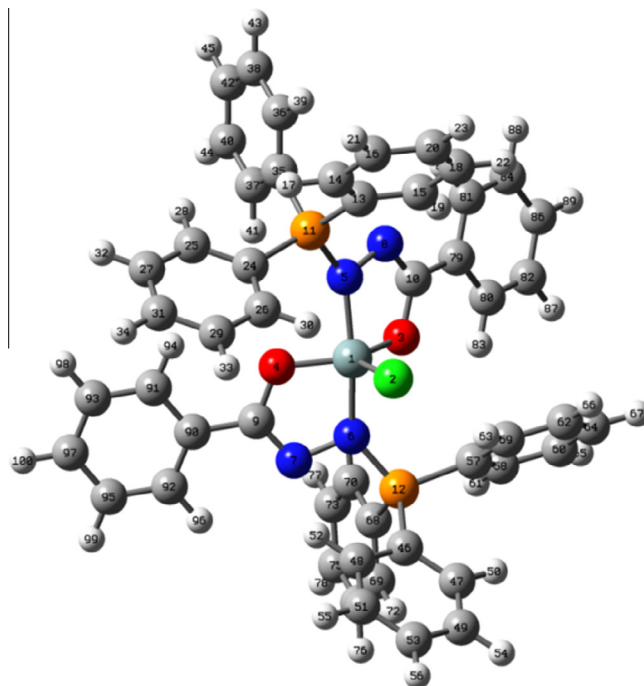


Fig. 3. DFT optimized structure of 3.

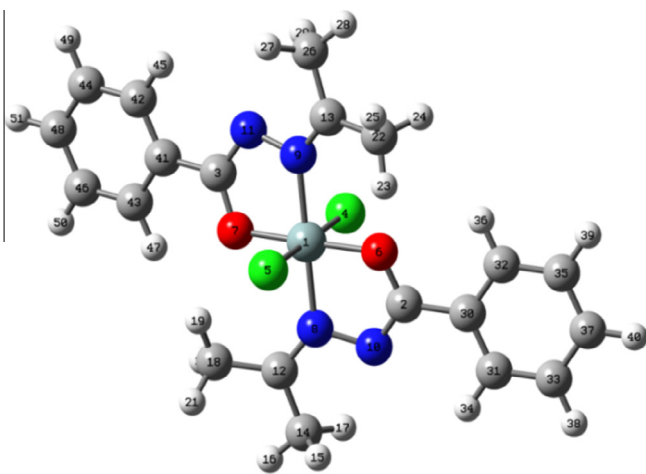


Fig. 2. DFT optimized structure of 2.

pentacoordinated silicon dichelate chloride (or bromide) salts, where Y = alkyl (**8–10**, **16**), phenyl (**11**, **17**) or halide (**12**, **13**), in high yield. All these products were characterized by their ^1H , ^{13}C , ^{29}Si and ^{31}P NMR spectral data. The structures of **8–13**, **16** and **17** were likewise obtained from their NMR spectral analyses and from the obvious analogy with the literature reports [26]. It is predicted that the geometry of **8–13**, **16** and **17** corresponds to a slightly distorted trigonal bipyramid (TBP), with nitrogen atoms occupying the axial positions.

Table 4 lists selected the multinuclear NMR data from the various spectra of the triphenylphosphinimino complexes. The ^{29}Si chemical shifts for the alkyl-substituted compounds (**8–13**, **16** and **17**) are all in the range -76 to -107 ppm, and they shift gradually to higher field as the ligands become more electron-withdrawing. All of these ^{29}Si chemical shifts are well within the range of characteristic pentacoordination and hence support the proposed ionic structures (Schemes 1 and 2).

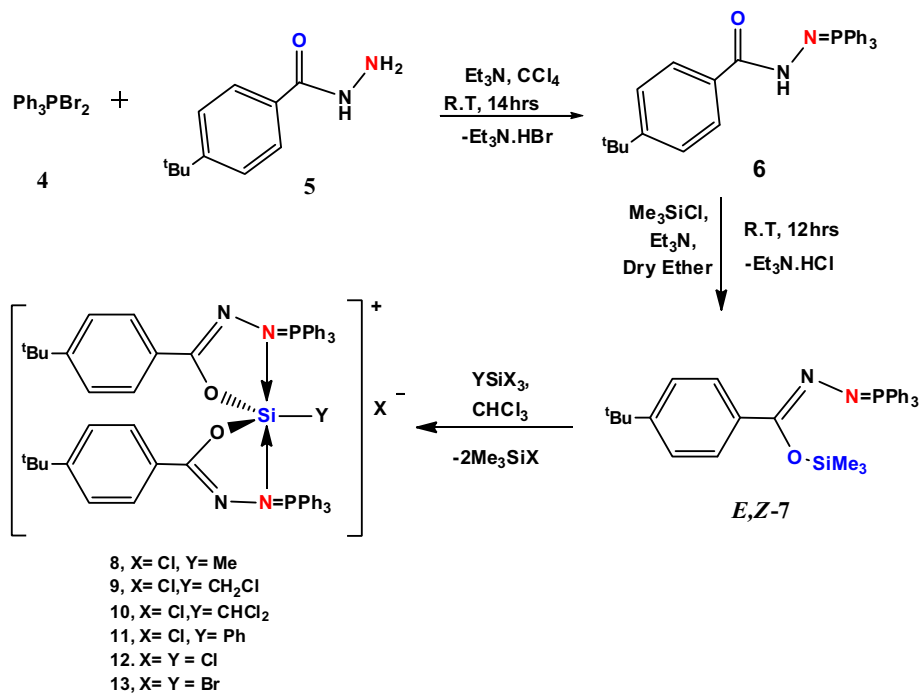
The fact that all of these new triphenylphosphinimino complexes are pentacoordinate in solution indicates that the donor ability of the new ligand is greater than those of the previously reported ligand systems **1** and **2**. The ionic nature of **8–13**, **16**

and **17** is further supported by the fact that they are insoluble in toluene, whereas essentially all of the neutral hexacoordinate silicon compounds studied to date are soluble in this solvent, as long as they do not ionize [27].

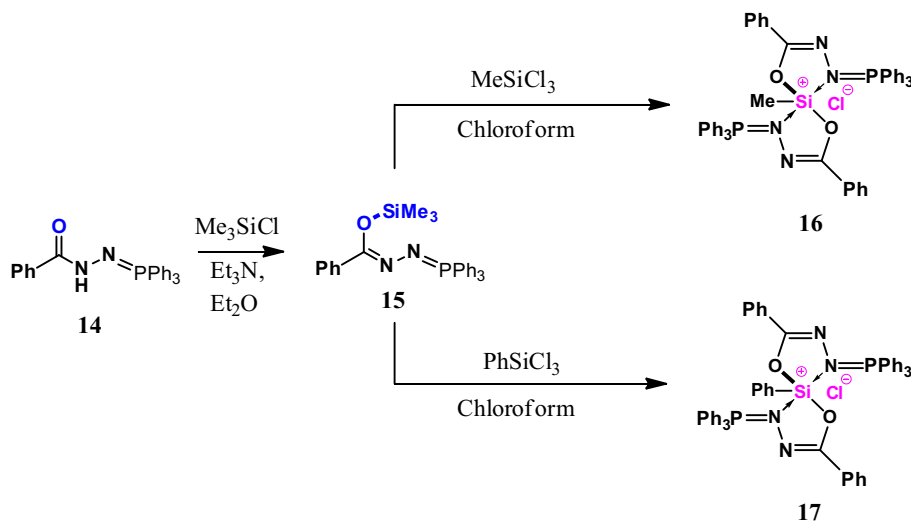
This interaction increases gradually in the compounds with the more electron-withdrawing ligands, **11–13**. It appears that in the presence of electron-withdrawing ligands coordination is stronger than in the alkyl complexes (**8–10**), as shown in Fig. 4. The effect of the Y ligands (Y = Me, Ph, CH_2Cl , CHCl_2 , Cl, Br and X = Cl or Br) on the ^{29}Si , ^{31}P and ^{13}C NMR chemical shifts is comparable with similar reported complexes [28].

The chemical shifts for YSiCl_3 were compared for the change in the ^{29}Si chemical shift of the complexes caused by coordination. The halogeno ligands attached directly to silicon (**12**, **13**) generate greater spin–spin interactions than the chloro- and dichloromethyl ligands (in **9** and **10**, respectively), in which carbon, and not halogen, is attached to silicon. It is interesting to note that the two-bond spin–spin interactions discussed above are of the same order of magnitude as those reported for similar interactions through covalent P–N–Si bonds [29].

It is worth determining the ^{29}Si NMR chemical shift because of its immense significance in expounding the identity of silicon possessing complexes. For this purpose the vapour and solvent phase ^{29}Si NMR chemical shifts of three pentacoordinated complexes were calculated, compared and contrasted with experimental values (Table 5). The experimentally observed chemical shift relative to TMS varies from -77 ppm to -106 ppm, however, the computed isotropic shifts range from -72 ppm to -84 ppm. It is obvious from the calculated results that there is a slight increase in the values of shielding constants in the presence of solvent. Although, the theoretical chemical shifts values mimic the experimental trend, a large deviation was observed depending upon various factors. One of the prime factors is the huge conformational flexibility and fluxionality of the complexes of interest (**8**, **11** and **13**). For complex **13**, the cumulative effect of conformational flexibility, fluxionality and spin orbit effects of the heavy atom for nuclear magnetic shifts of group 14 halides is accountable for the prevalent deviation of the studied complexes.



Scheme 1.



Scheme 2.

Table 4
 Significant NMR data of the complexes 8–13, 16 and 17.

Monodentate ligand (Y)	²⁹ Si NMR (δ in ppm)	³¹ P NMR (δ in ppm)	¹³ C NMR (δ in ppm) (C=N)
6 (free ligand)	–	29.57	168.63 (C=O)
7 (O-silylated)	7.6	16.24	151.23
8, Me	–77.07	36.43	155.33
9, CH ₂ Cl	–88.61	47.57	156.80
10, CHCl ₂	–94.09	53.20	158.67
11, Ph	–92.73	45.83	157.26
12, Cl	–99.02	49.80	157.78
13, Br	–106.24	53.14	158.03
14 (free ligand)	–	29.22	171.6
15 (O-silylated)	17.4	17.2	147.3
16, Me	–76.2	40.6	156.4
17, Ph	–94.3	47.3	157.6

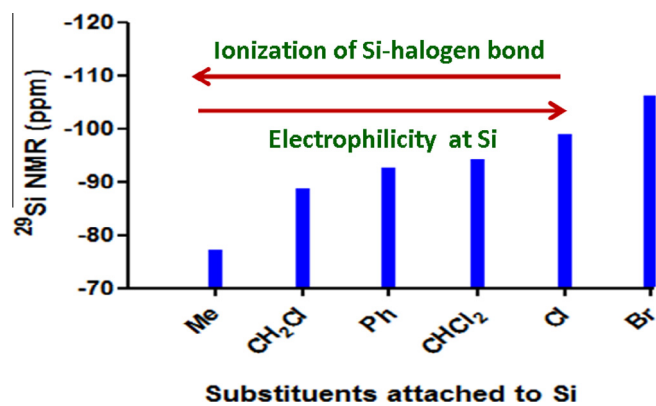
Fig. 4. Effect of Y group on the ²⁹Si NMR chemical shifts.

Table 5
Comparison of ^{29}Si NMR data for selected complexes.

Complex	Experimental ^{29}Si NMR (δ in ppm)	Calculated ^{29}Si -NMR (δ in ppm) Gs Phase	
8	-77.07	-72.06	-74.08
11	-92.73	-79.28	-82.90
13	-106.24	-83.69	-84.96

3.3. Ligand exchange reactions

Hypercoordinate silicon dichelates undergo two unique intermolecular chelate exchange reactions: (i) complete ligand transfer from dichelates to trichlorosilanes (PhSiCl_3) by a ligand priority order and (ii) bidentate ligand interchange between dichelates and a trimethylsilyl-hydrazide precursor. Evidence for complete intermolecular ligand crossover among different silicon(IV) complexes, further extending the flexible nature of these ligands and understanding the degree of coordination strength, is obtained.

3.3.1. Complete ligand transfer from the dichelates to PhSiCl_3 by a ligand priority order

The ligand crossover reactions were monitored in chloroform solutions by ^{29}Si and ^{31}P NMR (wherever necessary) spectral data. As shown in Eq. (1), addition of PhSiCl_3 to complex **16** readily gave a new complex (**17**) in chloroform solution. The data showed that PhSiCl_3 can easily attract the ligands from the silicon complex where $\text{X} = \text{Me}$. This was confirmed by obtaining two new signals in the ^{29}Si NMR spectrum at $\delta -12.4$ and -94.3 ppm for MeSiCl_3 and **17** respectively (Fig. 5). Subsequently the signals due to complex **16** and PhSiCl_3 disappeared. This could be due to the fact that the electron withdrawing Ph ring directly attached to silicon atom demands more electrons than the Me counterpart (**16**). This ligand crossover was not affected by the addition of neutral phosphine oxide or 1,10-phenanthroline ligands.

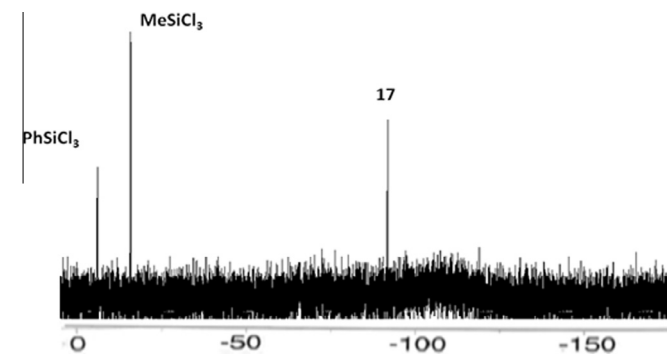


Fig. 5. ^{29}Si NMR spectral evidence for the formation of a new complex (**17**) by complete ligand transfer from **16** on addition of PhSiCl_3 .

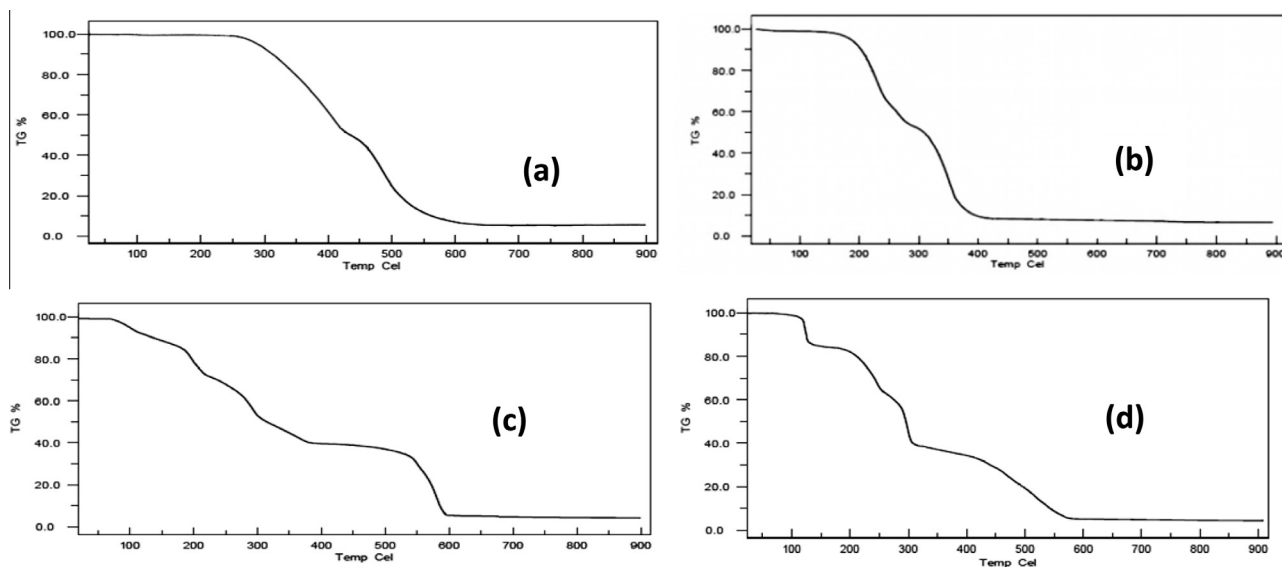
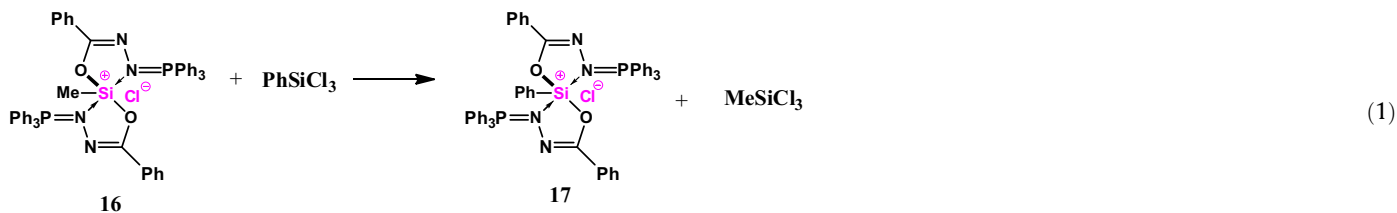
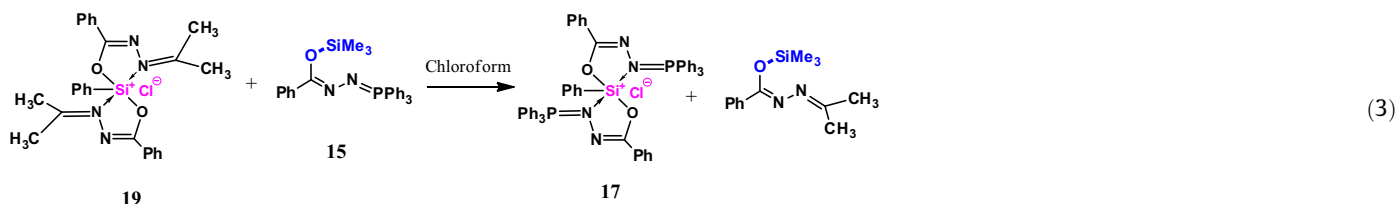
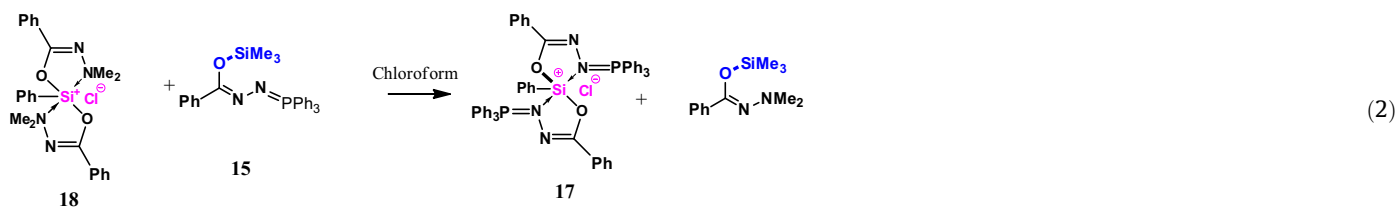


Fig. 6. TGA curves of hypercoordinated silicon(IV) complexes having Si-Me (a), Si-Ph (b), Si-Cl (c) and Si-Br (d) σ -bonds.

3.3.2. Bidentate ligand interchange between the dichelates and the trimethylsilyl-hydrazide precursor

When the ligand with the N=PPh₃ group (**15**) was added to **18**, containing –NMe₂ donor groups, the formation of **17** was observed immediately together with *O*-trimethylsilyl-*N*-(dimethylamino)benzohydrazide. This reaction is not reversible even with a large excess of *O*-trimethylsilyl-*N*-(triphenylphosphinimino)benzohydrazide. In a similar way, a noticeable exchange of two substituents involves complete removal of the bidentate chelating ligand from **19**, and its replacement by the ligand **15**. This clearly indicates the better donor ability of –N=PPh₃ ligand systems, as supported by DFT calculations.



3.4. Thermal analysis

The thermal behavior of the synthesized silicon(IV) complexes (**8**, **11–13**) at different temperatures was studied on the basis of TG/DTG and DTA data. Two stage thermal decomposition processes were observed on the TG curve for compound **8** (Fig. 6(a)). The first step of thermal decomposition was seen in the temperature range 158–300 °C with the release of two triphenylphosphine molecules in an exothermic effect, as shown in the DTA curve. The second step of the thermal decomposition, in the temperature range 300–370 °C, was found to be due to the removal of the remaining fragments of the ligand, as shown in Table 6. This was accompanied by an endothermic effect in the DTA curve. The final residual product of the thermal decomposition was found to be SiO₂. The proposed mechanism for the thermal decomposition of **8** is given in Scheme 3.

The thermal curve of compound **11** (Fig. 6(b)) was found to be similar to **8** within the temperature range 270–583 °C. The initial decomposition was observed in the temperature range 270–442 °C, due the loss of two molecules of triphenylphosphine with a mass loss of 51.4% (calc. 50.26%). The next stage of decomposition in the temperature range 442–583 °C was observed due to the removal of the remaining fragments of the ligand (Table 6), with a mass loss of 42.4% (calc. 43.98%), leaving the residue of 6.7% for SiO₂.

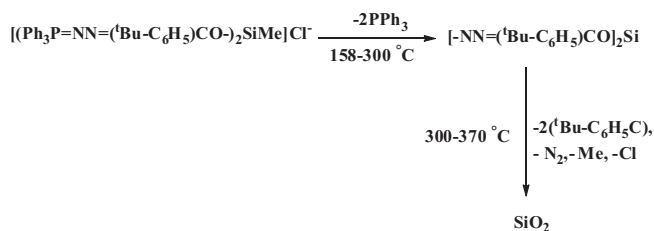
Complex **12** shows three major stages of thermal decomposition, as shown in the TG curve (Fig. 6(c)). The first stage could be due to the removal of two Cl atoms in the temperature range 80–120 °C, with a corresponding endothermic peak shown in the

DTA curve. The second step indicates the loss of two triphenylphosphine moieties in the temperature range 120–380 °C. The third step, in the relatively high temperature range 380–590 °C, corresponds to the thermal decomposition of the remaining fragment of the ligand into fragments (Table 2). Silicon dioxide was identified as the final residue. The proposed decomposition mechanism is shown in Scheme 4. The results of the thermal decomposition patterns of **13** (Fig. 6(d)) are similar to complex **12**.

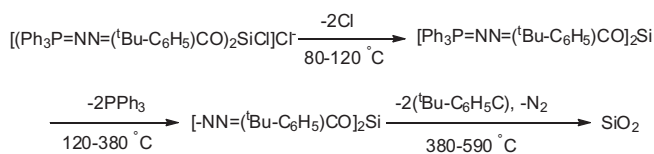
It is predicted that the TG curves of **12** and **13** reveal the loss of the ligand (XY) in the first step, with probable formation of an intermediate tetracoordinated silicon complex. The residual 4-(*t*-butyl)-*N*-(triphenylphosphoranylidene)benzohydrazide silicon compound decomposes finally to give SiO₂. Thermal stability follows the order: **8** (DTA 90 °C) < **11** (DTA 130 °C) < **12** (DTA 170 °C) < **13** (DTA 400 °C). In all the cases, the final residue was SiO₂ and it exactly matched the powder X-ray diffraction patterns of the literature reports.

Table 6
Thermolysis data of some selected hypercoordinate silicon(IV) complexes.

Compound	Stages of decomposition	TG temperature ranges/°C	Mass loss%		DTA curve	DTG max/°C	Assignment
			Calc.	Exp.			
8	First stage	158–300	50.4	52.1	Exo	124	2PPh ₃
	Second stage	300–372	42.8	40.8	Endo	275	2(<i>t</i> -Bu–C ₆ H ₅ C), N ₂ , Me, Cl
11	First stage	270–442	50.2	51.4	Exo	399	2PPh ₃
	Second stage	442–583	43.9	42.4	Exo	473	2(<i>t</i> -Bu–C ₆ H ₅ C), N ₂ , Ph, Cl
12	First stage	82–118	7.07	6.96		91	2Cl
	Second stage	120–381	52.4	50.2	Endo	187	2PPh ₃
	Third stage	381–592	34.6	35.4	Endo	582	2(<i>t</i> -Bu–C ₆ H ₅ C), N ₂
13	First stage	114–128	14.6	15.0	Endo	124	2Br
	Second stage	180–304	48.0	50.0	Endo	275	2PPh ₃
	Third stage	304–572	31.7	29.8	Endo	492	2(<i>t</i> -Bu–C ₆ H ₅ C), N ₂



Scheme 3.



Scheme 4.

4. Conclusions

Novel hypercoordinate silicon bis-chelate complexes with the phosphinimino-*N* ligand group have been prepared and characterized by multinuclear NMR spectroscopy. The phosphinimino-*N* ligand group is found to be superior in terms of strength of coordination to silicon through the formation of pentacoordinate silicon (IV) complexes relative to previously reported dimethylamino- and isopropylideneimino-coordinated analogous complexes. This superiority was further confirmed by ligand crossover reactions. The optimized DFT structures of some selected complexes closely agree with the experimental results through the bond lengths and bond angles of the respective silicon(IV) complexes. On thermolysis, the hypercoordinate silicon(IV) complexes containing a silicon-carbon σ -bond significantly undergo a two step decomposition, while the other complexes with silicon-halogen σ -bonds follow three steps. This clearly indicates the thermal decomposition strongly depends on the nature of the substituents directly attached to the central silicon atom. The controlled thermolysis of these complexes may give unusual transformations, leading to the preparation of novel silicon materials depending on the nature of ligand systems which are otherwise difficult to make. We are currently working on the bond making and bond breaking transformations of hypercoordinate silicon complexes.

Acknowledgments

Support for this work from DST-SERB, New Delhi, India (Ref. No. SR/Si/IC-38/2011) is gratefully acknowledged. Mr. Janardan Sannapaneni thanks DST for a fellowship and Mr. Suman Pothini is grateful to VIT University for a research associateship. Dr. A.S.R.K. and his group members thank DST-VIT-FIST for NMR and SIF-VIT University for other instrumentation facilities.

Appendix A. Supplementary data

Supplementary data associated with this article can be found, in the online version, at <http://dx.doi.org/10.1016/j.poly.2015.08.011>.

References

- [1] (a) S.K. Chopra, J.C. Martin, *J. Am. Chem. Soc.* 112 (1990) 5342; (b) R. Berger, K. Duff, J.L. Leighton, *J. Am. Chem. Soc.* 126 (2004) 5686; (c) C. Chuit, R.J.P. Corriu, C. Reye, J.C. Young, *Chem. Rev.* 93 (1993) 1371.

- [2] (a) J. Wagler, U. Böhme, E. Brendler, G. Roewer, *Organometallics* 24 (2005) 1348; (b) D. Kost, I. Kalikhman, *Adv. Organomet. Chem.* 50 (2004) 1; (c) D. Kost, V. Kingston, B. Gostevskii, A. Ellern, D. Stalke, B. Walfort, I. Kalikhman, *Organometallics* 21 (2002) 2293; (d) D. Kost, B. Gostevskii, N. Kocher, D. Stalke, I. Kalikhman, *Angew. Chem., Int. Ed.* 42 (2003) 1023; (e) D. Stalke, S. Deuerlein, N. Kocher, I. Kalikhman, D. Kost, *Organometallics* 24 (2005) 2913.
- [3] J. Wagler, T. Doert, G. Roewer, *Angew. Chem. Int. Ed.* 43 (2004) 2441.
- [4] J. Wagler, U. Böhme, G. Roewer, *Organometallics* 23 (2004) 6066.
- [5] S. Sergani, I. Kalikhman, S. Yakubovich, D. Kost, *Organometallics* 26 (2007) 5799.
- [6] S. Rendler, M. Oestreich, *Synthesis* 11 (2005) 1727.
- [7] Y. Orito, M. Nakajima, *Synthesis* 9 (2006) 1391.
- [8] (a) Reviews about the formation and structure of hypercoordinate silicon compounds S.N. Tandura, M.G. Voronkov, N.V. Alekseev, *Top. Curr. Chem.* 131 (1986) 99; (b) V.E. Shklover, Y.T. Struchov, M.G. Voronkov, *Russ. Chem. Rev.* 58 (1989) 211; (c) E. Lukevics, O. Pudova, R. Sturkovich (Eds.), *Molecular Structure of Organosilicon Compounds*, Ellis Horwood, Chichester, 1989; (d) R.R. Holmes, *Chem. Rev.* 96 (1996) 927.
- [9] (a) A. Hosomi, *Acc. Chem. Res.* 21 (1988) 200; (b) G.G. Furin, O.A. Vyazankina, B.A. Gostevsky, N.S. Vyazankin, *Tetrahedron* 44 (1988) 2675.
- [10] M. Benaglia, S. Guizzetti, L. Pignataro, *Coord. Chem. Rev.* 252 (2008) 492.
- [11] (a) H.H. Karsch, R. Richter, E. Witt, *J. Organomet. Chem.* 521 (1996) 185; (b) H.H. Karsch, R. Richter, E. Witt, in: N. Auner, J. Weis (Eds.), *In Organosilicon Chemistry III*, Wiley-VCH, Weinheim, Germany, 1997, p. 460; (c) U.-H. Berlekamp, P. Jutzi, *Angew. Chem. Int. Ed.* 38 (1999) 2048; (d) U.-H. Berlekamp, A. Mix, B. Neumann, H.-G. Stammeler, P. Jutzi, *J. Organomet. Chem.* 667 (2003) 167; (e) G. Muller, M. Waldkircher, A. Pape, in: N. Auner, J. Weis (Eds.), *In Organosilicon Chemistry III*, Wiley-VCH, Weinheim, Germany, 1997, p. 452.
- [12] C.C. Walker, H. Shechter, *J. Am. Chem. Soc.* 90 (1968) 5626.
- [13] G.B. Merrill, H. Shechter, *Tetrahedron Lett.* (1975) 4527.
- [14] (a) D. Kost, I. Kalikhman, M. Raban, *J. Am. Chem. Soc.* 117 (1995) 11512; (b) V. Kingston, B. Gostevskii, I. Kalikhman, D. Kost, *Chem. Commun.* (2001) 1272; (c) D. Kost, B. Gostevskii, N. Kocher, D. Stalke, I. Kalikhman, *Angew. Chem. Int. Ed.* 40 (2003) 1023; (d) B. Gostevskii, K. Adear, A. Sivaramakrishna, G. Silbert, D. Stalke, N. Kocher, I. Kalikhman, D. Kost, *Chem. Commun.* (2004) 1644; (e) Janardan, P. Suman, K. Vijayakrishna, A. Sivaramakrishna, *Synthesis and Reactivity in Inorganic, Metal-Organic and Nano-Metal Chemistry*, (2015) (in press); (f) I. Kalikhman, B. Gostevskii, A. Sivaramakrishna, D. Kost, N. Kocher, D. Stalke, in: *Steric Effect on the Formation, Structure and Reactions of Pentacoordinate Siliconium-Ion Salts*, in: N. Auner, J. Weis (Eds.), *Organosilicon Chemistry VI*, VCH-Wiley, Weinheim, 2008; (g) B. Gostevskii, G. Silbert, K. Adear, A. Sivaramakrishna, D. Stalke, S. Deuerlein, N. Kocher, M.G. Voronkov, I. Kalikhman, D. Kost, *Organometallics* 24 (2005) 2913.
- [15] (a) I. Kalikhman, B. Gostevskii, O. Girshberg, A. Sivaramakrishna, N. Kocher, D. Stalker, D. Kost, *J. Organomet. Chem.* 686 (2003) 202; (b) S. Janardan, P. Suman, K. Vijayakrishna, A. Sivaramakrishna, *Polyhedron* 85 (2015) 34; (c) B. Gostevskii, V. Pestunovich, I. Kalikhman, A. Sivaramakrishna, N. Kocher, S. Deuerlein, D. Leusser, D. Stalke, D. Kost, *Organometallics* 23 (2004) 4346.
- [16] M.J. Frisch, G.W. Trucks, H.B. Schlegel, G.E. Scuseria, M.A. Robb, J.R. Cheeseman, G. Scalmani, V. Barone, B. Mennucci, G.A. Petersson, *Gaussian 09 Revision A 02*, Gaussian, Wallingford CT, 2009.
- [17] A.D. Becke, *J. Chem. Phys.* 98 (1993) 5648.
- [18] C. Lee, W. Yang, R.G. Parr, *Phys. Rev. B* 37 (1988) 785.
- [19] S.H. Vosko, L. Wilk, M. Nusair, *Can. J. Phys.* 58 (1980) 1200.
- [20] E. Reed, R.B. Weinstock, F. Weinhold, *J. Chem. Phys.* 83 (1985) 735.
- [21] K.B. Wiberg, *Tetrahedron* 24 (1968) 1083.
- [22] R. Ditchfield, *Mol. Phys.* 27 (1974) 789.
- [23] M. Karni, Y. Apeloig, N. Takagi, S. Nagase, *Organometallics* 24 (2005) 6319.
- [24] J. Tomasi, B. Mennucci, R. Cammi, *Chem. Rev.* 105 (2005) 2999.
- [25] (a) P. Senthivell, M.N.S. Rao, J. Srinivas, G.S. Murthy, *Phosphorus, Sulfur, Silicon Relat. Elem.* 117 (1996) 179.
- [26] A. Sivaramakrishna, I. Kalikhman, E. Kertsnsus, A.A. Korlyukov, D. Kost, *Organometallics* 25 (2006) 3665.
- [27] (a) D. Schär, J. Belzner, in: N. Auner, J. Weis (Eds.), *In Organosilicon Chemistry III*, Wiley-VCH, Weinheim, Germany, 1997, p. 429; (b) I. Kalikhman, O. Girshberg, L. Lameyer, D. Stalke, D. Kost, *J. Am. Chem. Soc.* 123 (2001) 4700.
- [28] M.G. Voronkov, V.A. Pestunovich, Yu.I. Baukov, *Organomet. Chem. USSR* 4 (1991) 593.
- [29] B. Wrackmeyer, Eh. Kupče, G. Kehr, J. Schiller, *Magn. Reson. Chem.* 30 (1992) 304.